



Pulmonary Bone Cement Embolism: CT Angiographic Evaluation with Material Decomposition Using Gemstone Spectral Imaging

Sun Huh, MD, Heon Lee, MD, PhD

All authors: Department of Radiology, Soonchunhyang University Hospital Bucheon, Bucheon 420-767, Korea

We report a case of pulmonary bone cement embolism in a female who presented with dyspnea following multiple sessions of vertebroplasty. She underwent spectral CT pulmonary angiography and the diagnosis was made based on enhanced visualization of radiopaque cement material in the pulmonary arteries and a corresponding decrease in the parenchymal iodine content. Here, we describe the CT angiography findings of bone cement embolism with special emphasis on the potential benefits of spectral imaging, providing additional information on the material composition.

Index terms: Bone cement; Pulmonary embolism; Dual-energy CT; Spectral imaging

INTRODUCTION

Since it was first performed in 1984 by Galibert and Deramond (1), percutaneous vertebroplasty has become widely accepted as a minimally invasive procedure for the treatment of osteoporotic vertebral fractures and osteolytic malignant vertebral tumors. However, more complications associated with percutaneous vertebroplasty have been reported over time with increasing performance of this procedure. Among the various complications, the most serious is embolization of polymethylmethacrylate (PMMA) mixture, a commonly used cement material, in the pulmonary arteries (2, 3). In most cases, however, this event is asymptomatic. Thus, radiologists have a greater

chance of encountering cement emboli in postoperative patients undergoing chest CT for some unrelated reason (4).

Although postoperative chest radiography is performed to detect bone cement, the diagnosis of bone cement emboli is usually made with a chest CT (5). Typical CT findings include the presence of multiple tubular or branching dense opacities located along the course of the pulmonary arteries. However, dense opacified blood during contrast injection may mask the high-density bone cement emboli in some cases, and determining the functional significance of the emboli is not possible. Recently, CT pulmonary angiography (CTPA) with dual energy or spectral imaging mode was introduced to detect pulmonary thromboemboli and consequent perfusion defects in patients with dyspnea of unknown etiology, and, promisingly, it has been reported to result in significant improvements in the diagnostic performance of CTPA (6-8). We performed CTPA with spectral mode in a patient with dyspnea and describe the CT findings of bone cement embolism with special emphasis on the potential benefits of the spectral imaging mode. To our knowledge, this is the first report to describe spectral CT angiographic findings in a patient with pulmonary bone cement embolism. This study was approved by the Institutional Review Board.

Received March 6, 2014; accepted after revision May 8, 2014.
This work was supported by Soonchunhyang University research fund.

Corresponding author: Heon Lee, MD, PhD, Department of Radiology, Soonchunhyang University Hospital Bucheon, 170 Jomaru-ro, Wonmi-gu, Bucheon 420-767, Korea.

• Tel: (8232) 621-5851 • Fax: (8232) 621-5874
• E-mail: acarad@naver.com

This is an Open Access article distributed under the terms of the Creative Commons Attribution Non-Commercial License (<http://creativecommons.org/licenses/by-nc/3.0>) which permits unrestricted non-commercial use, distribution, and reproduction in any medium, provided the original work is properly cited.

CASE REPORT

A 56-year-old woman was admitted for intermittent dyspnea and hypotension. She had undergone seven previous vertebroplasties at another hospital for the treatment of the compression fractures due to severe osteoporosis, with a bone mineral density T-score of -3.4. She developed dyspnea 6 months after her last surgery.

On arrival, her blood pressure was 80/50 mm Hg; however, blood gas analysis revealed normal oxygenation status. A chest radiograph showed multiple tubular, radiopaque lesions corresponding to the course of the pulmonary vascular structures. CTPA was then performed using gemstone spectral imaging (GSI) to obtain spectral CT images by fast kV switching, which allows for virtual monochromatic images at different kV levels from 40 to 140 keV and the creation of material density images. An axial

maximal intensity projection image using 140 kVp revealed radiopaque emboli of variable sizes and shapes in the lobar, segmental, and subsegmental pulmonary arteries of the right upper, middle, and both lower lobes (Fig. 1A). Additionally, images with a mediastinal setting demonstrated the origin of the leak by showing cement in right laterovertebral vein at the level of the third and fifth lumbar vertebral bodies, draining into the inferior vena cava and right common iliac vein. A small amount of asymptomatic cement leakage in the epidural space of the fifth to the eighth thoracic, first lumbar, and third lumbar vertebrae and a needle tract at the sixth thoracic vertebral level were also detected (Fig. 1B). There was no characteristic finding of pulmonary infarction, such as pleural-based truncated consolidation or ground-glass opacities.

Iodine maps were created using the GSI software (AW Gemstone spectral imaging, GE Medical Systems, Milwaukee,

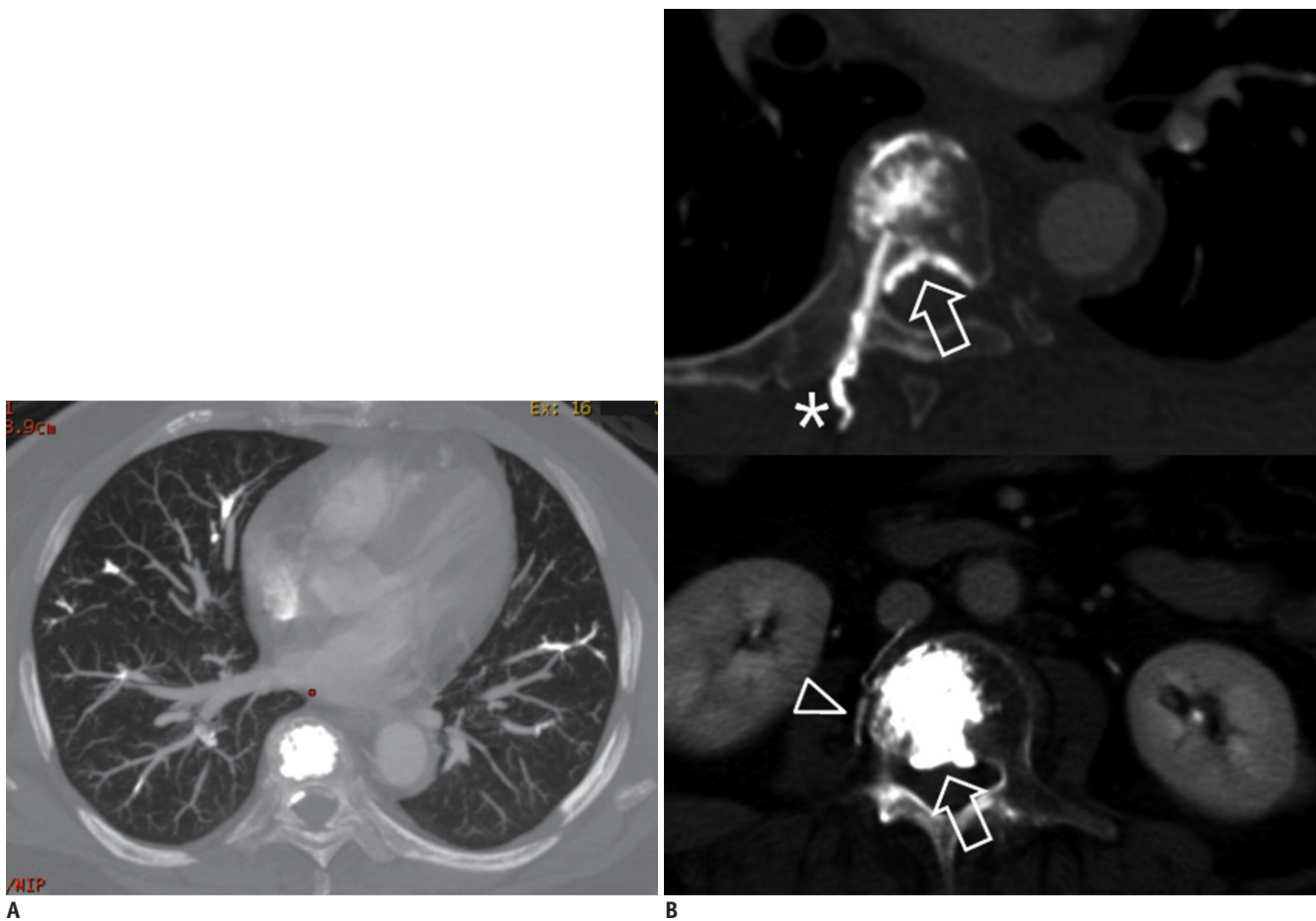


Fig. 1. Spectral CT angiography of 56-year-old woman admitted for intermittent dyspnea and hypotension.
A. Axial maximal-intensity projection (MIP) image from monochromatic reconstruction at 140 kVp revealed bone cement emboli of variable sizes and shapes in lobar, segmental, and subsegmental pulmonary arteries of right middle and both lower lobes. This MIP image was reconstructed at 10-mm thickness. **B.** Multiplanar reconstruction images showed multifocal epidural cement leakage in epidural spaces at thoracic and lumbar vertebral levels (arrows). Bone cement extended to back muscle through needle tract (*) at sixth thoracic vertebral level (upper). Axial image at level of third lumbar vertebral body demonstrated origin of leak, showing cement in right laterovertebral vein (arrowhead).

Spectral CTA of Pulmonary Bone Cement Embolism

WI, USA). An axial iodine material density image at the same level shown in Figure 1A more clearly demonstrated the smaller segmental and subsegmental emboli and the corresponding decrease in the parenchymal iodine content (Fig. 1C). These images also showed the under-perfused areas in the right middle lobe and lingular division of the left upper lobe that correlated with the embolic-

occluded pulmonary arterial vascular territory (Fig. 1D), which was not visible on the monochromatic CTPA image for morphological assessment of the pulmonary artery (Fig. 1A). A GSI scatter plot and histograms (Fig. 1E, F) for material separation showed that the pulmonary emboli and bone cement in the vertebral body were similar in composition. However, the cortical bone, bone cement

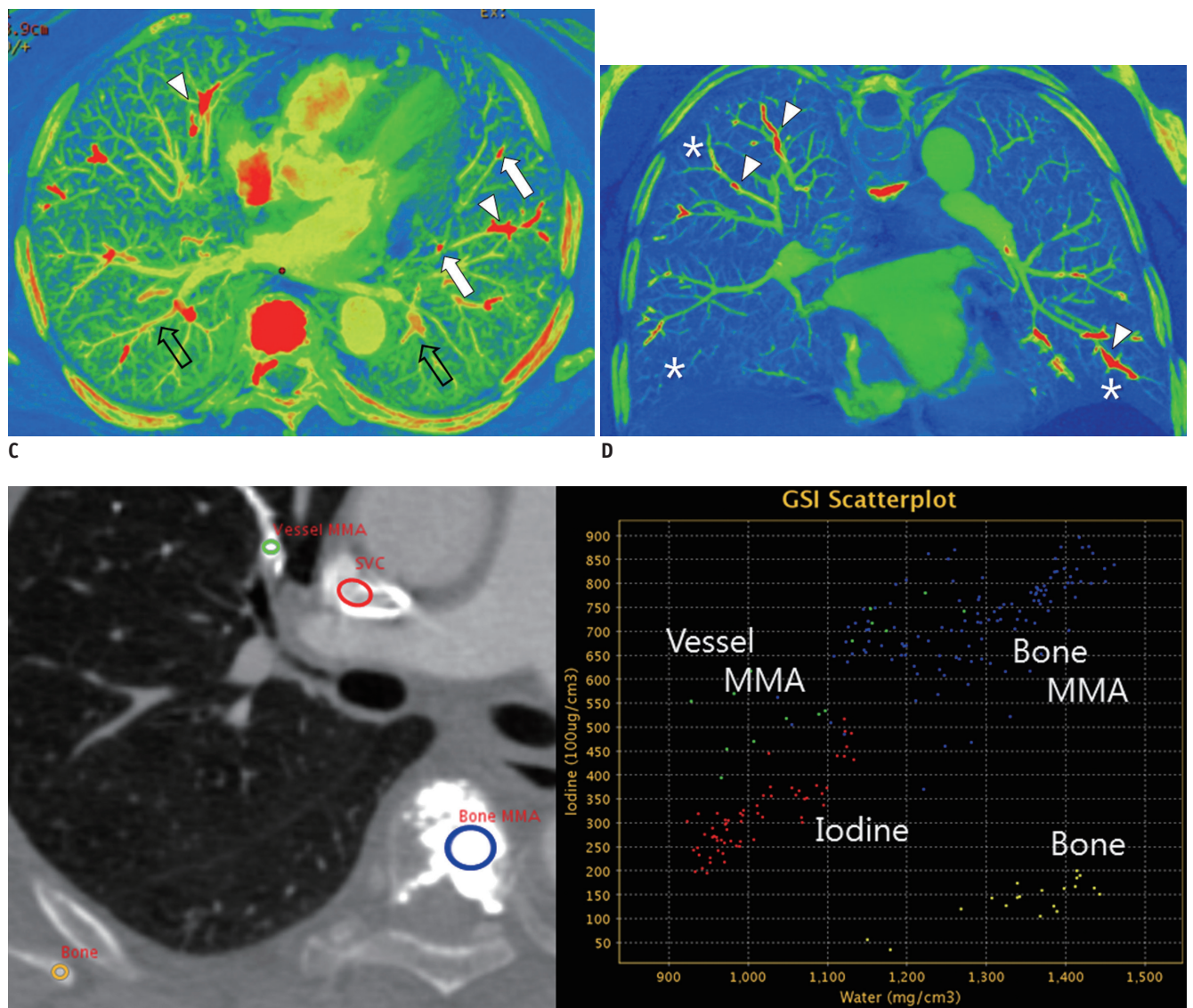
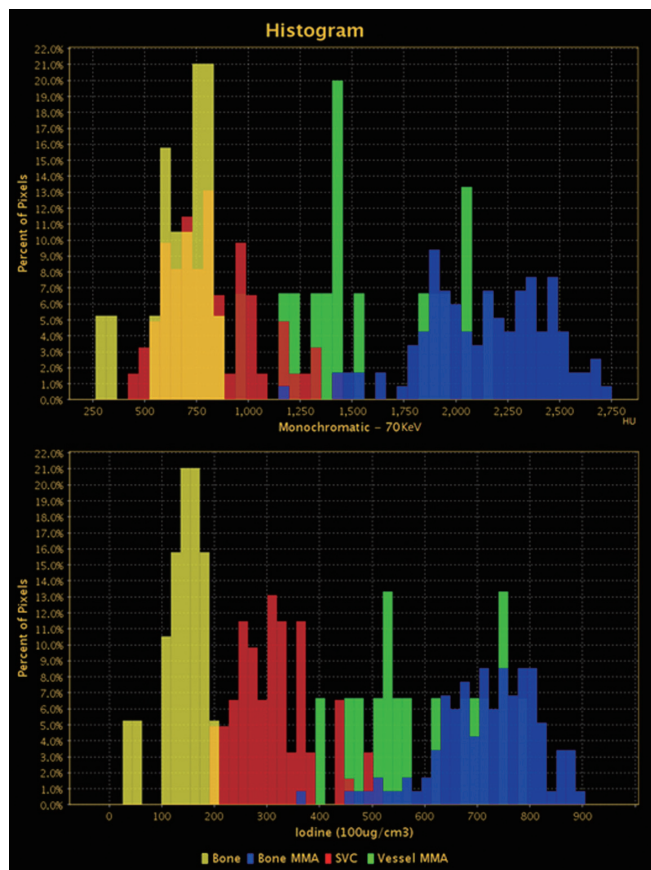


Fig. 1. Spectral CT angiography of 56-year-old woman admitted for intermittent dyspnea and hypotension.
C. Axial iodine, material-density image (iodine map) created from gemstone spectral imaging (GSI) software at same level shown in Figure 1A demonstrated multiple pulmonary cement emboli in red (arrowheads) and corresponding decrease in parenchymal iodine content. Compared with Figure 1A, iodine map more clearly demonstrated smaller bone cement-emboli in segmental and subsegmental arteries (arrows). Note amorphous pink casts (open arrows) in multiple pulmonary arterial branches, shown to be dense iodinated blood, not cement materials, on GSI scatter plot (data not shown). **D.** Iodine map reconstructed in oblique coronal plane, passing from posterosuperior to anteroinferior, allowed direct visualization of embolic materials within pulmonary arteries (arrowheads). Corresponding underperfused area (*) correlated with embolic-occluded pulmonary arterial vascular territory. **E.** Gemstone spectral imaging (GSI) scatter plot for material separation showed similar compositions of pulmonary emboli and bone cement in vertebral body. However, it demonstrated that bone, bone cement, and iodinated contrast in this patient had different compositions although all of them show similar high attenuation in monochromatic image. Iodine, bone, and bone cement were represented on iodine (water) material density pairs using GSI scatter plot.



F
Fig. 1. Spectral CT angiography of 56-year-old woman admitted for intermittent dyspnea and hypotension.

F. Hounsfield unit (upper) and iodine content (lower) histograms of region of interest in Figure 1E. In this case, iodinated contrast had overlapping density with bone and cement emboli on Hounsfield unit based histogram created from 70 KeV monochromatic spectral energy (upper). However, in iodine content histogram (lower), these materials were clearly separated. Furthermore, positions of pulmonary embolus and vertebral bone cement showed considerable overlap, suggesting that these two materials had identical or similar compositions and that pulmonary embolus had originated from cement material in vertebral body.

in the vertebral body, and iodine being assessed in this patient were different in composition from one another, although all of them showed high attenuation similarly on the monochromatic image.

After administration of inotropics, the patient's blood pressure normalized, and she was transferred to another community hospital for further anticoagulation treatment.

DISCUSSION

Although percutaneous vertebroplasty is considered to be a minimally invasive procedure, many local and systemic complications can occur. Cement leakage is the most

frequent complication after percutaneous vertebroplasty caused by injecting PMMA mixture (approximately 90% MMA and 10% barium sulfate) when it is still too liquid in state or by applying too much pressure while injecting the material (2). Although there is a high prevalence of extravertebral cement leakage into the surrounding venous plexus after vertebroplasty, only a small percentage of cement leakage leads to pulmonary embolism (3). The present case showed that the cement leaked into the right laterovertebral veins and was drained by the inferior vena cava via which the cement migrated to the pulmonary arteries.

Traditional imaging tools for the diagnosis of pulmonary embolism include invasive pulmonary angiography, nuclear ventilation/perfusion scans, and, more recently, CTPA. Although chest radiography can be used as a screening tool, CTPA is widely accepted as the standard for the diagnosis of pulmonary embolism by direct visualization of emboli within a pulmonary artery (5). However, while CTPA is known to be highly accurate for the detecting thromboemboli in the central pulmonary vessels, its sensitivity decreases near the periphery, where the vessels are smaller and there is a higher chance of motion artifacts caused by breathing. The CT detectability of subsegmental pulmonary thrombi is variable, with a sensitivity ranging from 37 to 96% (9). Furthermore, while multidetector CT (MDCT) technology has better spatial resolution and a lower scan time than those of traditional diagnostic tools, the lack of functional data obtained from CT often requires the use of additional nuclear imaging studies to visualize perfusion defects, especially with chronic smaller emboli (9). The ongoing evolution in MDCT technology has resulted in dual-source, dual-energy CT or single-source spectral CT with rapid tube voltage switching, which allow for iodine mapping of the lung field on post-contrast CT studies and the detection of decreased iodine content (perfusion defects) distal to obstructive clots (6-8). Initial studies evaluated the diagnostic accuracy of the perfusion map generated using dual-energy CT and spectral CT imaging and showed promising results for the detection of blood clots. In those studies, the detection performance of blood clots, especially in smaller segmental and subsegmental arteries, could be improved not by direct visualization of clots but rather with simultaneous evaluation of iodine perfusion maps (6).

However, in contrast to those studies, spectral CT imaging in the present case improved the direct visualization of tiny radiopaque cement materials in smaller segmental

and peripheral subsegmental arterial branches that were masked by iodinated contrast materials in the pulmonary arteries (Fig. 1A, C). Furthermore, as shown in Figure 1E and F, spectral imaging allowed for the creation of material decomposition images, which may provide additional information on the material composition, based on the attenuation physics (8). This enabled estimating the different compositions of high-density materials, including iodinated contrast, bone, and cement, using material separation and spectral scatter plots. We believe that this may help to overcome the limitations associated with using only Hounsfield units and morphology to differentiate materials. In this case, the positions of the emboli in the pulmonary arteries and cement in the vertebral bodies overlapped each other on the GSI scatter plots and the histograms, suggesting that these two materials have identical or similar compositions, and that the pulmonary emboli originated from cement material in the vertebral body. Thus, we believe that spectral imaging may be useful in patients with both bone cement embolism as well as "classic" thromboembolism, although further studies involving more cases are needed. Furthermore, spectral imaging may have potential benefits for the early diagnosis of minor small, peripheral emboli to guide a follow-up plan in asymptomatic patients.

The indications for treatment in this setting have not been studied fully. In previous reports, most patients with asymptomatic cement embolism remained untreated. In symptomatic patients, however, anticoagulation therapy was started immediately to prevent further thrombus formation although there are no data supporting the value of preventive anticoagulation (4).

In conclusion, we performed pulmonary CTA in a patient with bone cement embolism using the spectral imaging mode. Spectral imaging allowed for better detection of smaller emboli even in the peripheral pulmonary arteries,

as well as evaluation of parenchymal perfusion by assessing the parenchymal iodine content in addition to angiographic information. Furthermore, we believe that the use of the material decomposition technique with spectral CT may help to compensate for the drawbacks of using only Hounsfield units in differentiating materials with similar CT densities.

REFERENCES

1. Galibert P, Deramond H, Rosat P, Le Gars D. [Preliminary note on the treatment of vertebral angioma by percutaneous acrylic vertebroplasty]. *Neurochirurgie* 1987;33:166-168
2. Krueger A, Bliemel C, Zettl R, Ruchholtz S. Management of pulmonary cement embolism after percutaneous vertebroplasty and kyphoplasty: a systematic review of the literature. *Eur Spine J* 2009;18:1257-1265
3. Barragán-Campos HM, Vallée JN, Lo D, Cormier E, Jean B, Rose M, et al. Percutaneous vertebroplasty for spinal metastases: complications. *Radiology* 2006;238:354-362
4. Choe DH, Marom EM, Ahrar K, Truong MT, Madewell JE. Pulmonary embolism of polymethyl methacrylate during percutaneous vertebroplasty and kyphoplasty. *AJR Am J Roentgenol* 2004;183:1097-1102
5. Remy-Jardin M, Pistolesi M, Goodman LR, Gefter WB, Gottschalk A, Mayo JR, et al. Management of suspected acute pulmonary embolism in the era of CT angiography: a statement from the Fleischner Society. *Radiology* 2007;245:315-329
6. Lu GM, Wu SY, Yeh BM, Zhang LJ. Dual-energy computed tomography in pulmonary embolism. *Br J Radiol* 2010;83:707-718
7. Lu GM, Zhao Y, Zhang LJ, Schoepf UJ. Dual-energy CT of the lung. *AJR Am J Roentgenol* 2012;199(5 Suppl):S40-S53
8. Sun YS, Zhang XY, Cui Y, Tang L, Li XT, Chen Y, et al. Spectral CT imaging as a new quantitative tool? Assessment of perfusion defects of pulmonary parenchyma in patients with lung cancer. *Chin J Cancer Res* 2013;25:722-728
9. Ghaye B. Peripheral pulmonary embolism on multidetector CT pulmonary angiography. *JBR-BTR* 2007;90:100-108